

*OsteoArthritis and Cartilage* (2006) 14, 1227–1236

© 2006 OsteoArthritis Research Society International. Published by Elsevier Ltd. All rights reserved.

doi:10.1016/j.joca.2006.05.013

# Osteoarthritis and Cartilage

**International  
Cartilage  
Repair  
Society**

## The effects of TGF- $\beta$ 1 and IGF-I on the biomechanics and cytoskeleton of single chondrocytes

N. D. Leipzig Ph.D., S. V. Eleswarapu B.S.E.N.G. and K. A. Athanasiou P.E., Ph.D.\*

*Department of Bioengineering, Rice University, Houston, Texas, USA*

### Summary

**Objective:** Ascertaining how mechanical forces and growth factors mediate normal and pathologic processes in single chondrocytes can aid in developing strategies for the repair and replacement of articular cartilage destroyed by injury or disease. This study examined effects of transforming growth factor- $\beta$ 1 (TGF- $\beta$ 1) and insulin-like growth factor-I (IGF-I) on the biomechanics and cytoskeleton of single zonal chondrocytes.

**Method:** Superficial and middle/deep bovine articular chondrocytes were seeded on tissue culture treated plastic for 3 and 18 h and treated with TGF- $\beta$ 1 (5 ng/mL), IGF-I (100 ng/mL), or a combination of TGF- $\beta$ 1 (5 ng/mL) + IGF-I (100 ng/mL). Single chondrocytes from all treatments were individually studied using viscoelastic creep testing and stained with rhodamine phalloidin for the F-actin cytoskeleton. Lastly, real-time RT-PCR was performed for  $\beta$ -actin.

**Results:** Creep testing demonstrated that all growth factor treatments stiffened cells. Image analysis of rhodamine phalloidin stained chondrocytes showed that cells from all growth factor groups had significantly higher fluorescence than controls, mirroring creep testing results. Growth factors altered cell morphology, since chondrocytes exposed to growth factors remained more rounded, exhibited greater cell heights, and were less spread. Finally, real-time RT-PCR revealed no significant effect of growth factor exposure on  $\beta$ -actin mRNA abundance. However,  $\beta$ -actin expression varied zonally, suggesting that this gene would be unsuitable as a PCR housekeeping gene.

**Conclusions:** These results indicate that TGF- $\beta$ 1 and IGF-I increase F-actin levels in single chondrocytes leading to stiffening of cells; however, there does not appear to be direct transcriptional regulation of unpolymerized  $\beta$ -actin. This suggests that the observed response is most likely due to signaling cross-talk between growth factor receptors and integrin/focal adhesion complexes.

© 2006 OsteoArthritis Research Society International. Published by Elsevier Ltd. All rights reserved.

**Key words:** Chondrocyte, Growth factors, Creep testing, Actin cytoskeleton, Fluorescence microscopy, Real-time RT-PCR.

### Introduction

Existing research has highlighted the need for the complete characterization of cellular milieu, especially toward understanding the processes of mechanotransduction in native and engineered tissues. Such knowledge would foster understanding of mechanical forces and their role in cell and tissue function. It would also be vital to elucidating disease etiologies, as well as the processes of formation and regeneration in tissues. In terms of tissue engineering, this knowledge would provide insight into the forces required for directing cells toward growing functional tissues *in vitro*.

Articular cartilage has been chosen as a leading target for tissue engineering for the simple fact that one in five adults experience significant morbidity due to cartilage injury and disease. Furthermore, articular cartilage engineering may appear to be an easy problem to tackle, considering that the tissue is avascular and contains very few cells. However, the tissue has a complex structure, exhibits a high degree of heterogeneity, and functions under an intensely strenuous environment. Articular cartilage is normally divided into four zones: superficial, middle, deep, and calcified. As reviewed<sup>1</sup>, each zone has distinct differences in

extracellular matrix (ECM) distribution, biosynthesis, gene expression, cell morphology, and physical properties.

Tissue engineering of cartilage thus far has proven unsuccessful in terms of replicating a fully functional tissue capable of withstanding the strenuous biomechanical environment within synovial joints. So far researchers have revealed that two stimuli, mechanical forces and chemical signals, seem to be important for influencing cartilage tissue formation, as well as its disease pathways. Studies with explants and chondrocytes have demonstrated that specific regimens of hydrostatic pressure, compression, and fluid forces can induce positive changes in gene expression and matrix synthesis<sup>2–7</sup>, while other regimens, namely static loads, can induce degenerative changes<sup>3,6</sup>. However, the precise levels of mechanical stimulation necessary to elicit chondrocyte response to mechanical loading are not clearly understood. A variety of growth factors and cytokines have been studied for their potential use in stimulating articular cartilage regeneration. Two growth factors have shown the most promise as demonstrated by stimulation of matrix synthesis, increased proliferation, and maintenance of phenotype: transforming growth factor- $\beta$ 1 (TGF- $\beta$ 1)<sup>8–12</sup> and insulin-like growth factor-I (IGF-I)<sup>13–18</sup>. It has also been shown that these growth factors can have synergistic effects when treating chondrocytes<sup>19</sup>.

Previous research demonstrates the tremendous promise growth factors have shown for influencing cells toward tissue formation<sup>8–19</sup>. Most cartilage or chondrocyte based studies have analyzed the response of explants or large

\*Address correspondence and reprint requests to: Kyriacos A. Athanasiou, Department of Bioengineering, MS-142, P.O. Box 1892, Rice University, Houston, TX 77251-1892, USA. Tel: 1-713-348-6395; Fax: 1-713-348-5877; E-mail: [athanasiou@rice.edu](mailto:athanasiou@rice.edu)

Received 10 October 2005; revision accepted 13 May 2006.

populations of cells. These studies are important for understanding physiological responses of cartilage, but they neglect to account for variations among either single cells or subpopulations of cells. Thus, it is necessary to take a reductionist approach by first studying single chondrocyte physiology to fully understand how cell responses translate to overall cartilage responses<sup>20</sup>. We are specifically interested in examining how growth factors influence single chondrocytes and how mechanical forces can modify these responses.

To date, several groups have attempted to describe cell signaling after TGF- $\beta$ 1 and IGF-I treatment. These studies have focused on signaling between TGF- $\beta$ 1 and IGF-I growth factor receptors and integrins<sup>21–23</sup>. The process of integrin activation in conjunction with IGF-I stimulation has been linked to the activation of signaling intermediates in several cell types. One such study demonstrated that chondrocytes plated on type I or type II collagen followed by IGF-I stimulation resulted in association of focal adhesion kinase (FAK) with  $\beta$ 1 integrins, vinculin, and paxillin, as well as induction of greater Shc (adaptor protein) expression<sup>23</sup>. It was postulated that IGF-I receptors cooperate with integrins to regulate focal adhesion proteins and are linked to the mitogen-activated protein kinase (MAPK) signaling pathway by a common Shc-growth factor bound protein 2 (GRB2) intermediate. TGF- $\beta$ 1 stimulation has also been tied to integrin activation in chondrocytic cells. For example, one study has shown that TGF- $\beta$ 1 stimulation and  $\alpha$ 2 $\beta$ 1 integrin activation (by type II collagen stimulation) led to synergistic increases in the phosphorylation of Smad2 and Smad3<sup>22</sup>. The signaling between TGF- $\beta$ 1 and integrins was demonstrated to occur before Smad phosphorylation. It has also been demonstrated that inhibiting FAK decreases cell attachment and blocks integrin signaling<sup>21</sup>.

Before one can hope to describe the mechanotransductive processes occurring *in vivo* and *in vitro* in native and engineered cartilage, a better understanding of individual chondrocyte behavior is necessary. We have previously described the development of devices able to mechanically test single adherent chondrocytes and osteoblasts<sup>24–26</sup> for determining their mechanical properties. The most recent setup of our device utilizes unconfined creep compression on single cells<sup>26</sup>.

The overall objective of this study was to determine what effects TGF- $\beta$ 1 and IGF-I would have on the mechanical properties of single articular chondrocytes, temporally and as a function of zone. The primary goal of this study was to quantify biomechanical alterations in single chondrocytes pertinent toward tissue regeneration or the etiology of disease states. Understanding a single chondrocyte's biomechanical response to static compression has implications toward understanding the forces responsible for initiating both anabolic and catabolic changes in cartilage. Based on the known actions of TGF- $\beta$ 1 and IGF-I<sup>8–19,21–23</sup>, our hypothesis was that these growth factors would lead to preservation of a more rounded chondrocytic phenotype. Based on previous work, we expected to observe differences between zones<sup>27</sup>, growth factor treatments<sup>8–19,21–23</sup>, and possible synergistic effects between TGF- $\beta$ 1 and IGF-I<sup>19</sup>. For this study we used single cell unconfined creep compression, fluorescence microscopy, and real-time reverse transcriptase-polymerase chain reaction (RT-PCR) to determine what effects the growth factors TGF- $\beta$ 1 (5 ng/mL), IGF-I (100 ng/mL), and a combination of TGF- $\beta$ 1 (5 ng/mL) and IGF-I (100 ng/mL), would have on zonal chondrocytes after 3 and 18 h of attachment.

## Method

### CELL CULTURE

Articular cartilage was obtained from the distal metatarsal joint of approximately 18-month-old steers obtained from local abattoirs. Chondrocyte harvest, isolation, and culture followed previously described protocols<sup>26</sup>. Briefly, the superficial and middle/deep zones were separated and digested overnight at 37°C and 10% CO<sub>2</sub> in a solution of 2 mg/mL collagenase type 2 (Worthington Biochemical, Lakewood, NJ) in supplemented Dulbecco's modified Eagle medium (DMEM) containing 10% fetal bovine serum (FBS), 100 U/mL penicillin–streptomycin, 0.25  $\mu$ g/mL fungizone, and 0.1 mM non-essential amino acids (NEAA) (Invitrogen Life Technologies, Carlsbad, CA). After digestion, the cell mixture was centrifuged and resuspended in supplemented DMEM. The cell suspension was seeded onto a tissue culture treated plastic (TCP) 150  $\times$  20 mm dish (plasma treated by Techno Plastic Products, Trasadingen, Switzerland) and confined to a 2 cm diameter area using silicone isolators (PGC Scientifics, Gaithersburg, MD) to yield an areal cell density of approximately  $3.3 \times 10^4$  cells/cm<sup>2</sup>. The plates were incubated for either 3 or 18 h at 37°C and 10% CO<sub>2</sub> prior to compression testing. These seeding times were selected such that we could characterize cellular events occurring immediately after attachment. Three hours is usually the approximate time that cells begin attaching. Cells are more firmly attached by the overnight, 18 h time point.

### GROWTH FACTOR TREATMENT

The growth factors TGF- $\beta$ 1 and IGF-I were selected for this study. These growth factors were used at a single concentration each, based on high or saturation values found in the literature<sup>8–19</sup>. For TGF- $\beta$ 1 and IGF-I, concentrations of 5 ng/mL and 100 ng/mL, respectively, were selected for experimentation. A third growth factor treatment was selected using a combination of TGF- $\beta$ 1 and IGF-I at a concentration of 5 ng/mL and 100 ng/mL, respectively. Both growth factors were obtained from PeproTech Inc. (Rocky Hill, NJ). For both cell seeding times (3 and 18 h), cells were exposed to the appropriate growth factor for the final 3 h of attachment. The design of this experiment is presented in Table I.

### SINGLE CELL CREEP TESTING

Unconfined creep compression tests were performed using a system developed in our laboratory, originally designed for displacement-controlled indentation testing of single cells<sup>24</sup>. Since its original design, this device has been modified first for indentation creep testing<sup>25</sup> and finally for the purpose of unconfined creep testing<sup>26</sup>. This device is designed to apply a constant stress on adherent cells while employing cantilever beam theory to track the resulting cellular deformation. Single cell unconfined compression is achieved by the application of a 50.8  $\mu$ m diameter tungsten probe (Advanced Probing, Boulder, CO).

After cell attachment, the media were removed from the culture dish and replaced with supplemented media containing 30 mM 4-(2-hydroxyethyl)-1-piperazineethanesulfonic acid (HEPES) buffer (Fisher Scientific, Pittsburgh, PA) warmed to 37°C to buffer pH changes when moving to ambient conditions. TGF- $\beta$ 1, IGF-I, or the combination of TGF- $\beta$ 1 and IGF-I was included in the fresh media for the corresponding treatment group. The dish was then placed into the apparatus and maintained at ambient conditions for creep testing.

Table I  
Experimental design showing all treatments yielding a total of 16 groups

Attachment time	Zone	Growth factor treatment
3 h	Superficial	Control
		TGF- $\beta$ 1
		IGF-I
	Middle/deep	TGF- $\beta$ 1 + IGF-I
		Control
		TGF- $\beta$ 1
18 h	Superficial	IGF-I
		TGF- $\beta$ 1 + IGF-I
		Control
	Middle/deep	TGF- $\beta$ 1
		IGF-I
		TGF- $\beta$ 1 + IGF-I
Growth factor exposure for entire 3 h of seeding (except for control)		
15 h seeding followed by 3 h of growth factor exposure (except for control)		

Creep testing was performed as described previously<sup>26</sup>. Briefly, single cells were creep tested using a test load of 50 nN. This test load was lower than what was previously used and resulted in cellular strains at or below 30% to conform to continuum model assumptions. The contact stress for each cell was determined via reticle measurement (Nikon USA, Melville, NY) of the cell diameter before compression. Contact stress was calculated by dividing the test load by the area of the cell. Cell height was determined by comparing probe contact with the cell to the measured distance to the dish.

#### DETERMINATION OF SINGLE CHONDROCYTE MATERIAL PROPERTIES

The creep response of single chondrocytes to unconfined compression was modeled using a closed-form continuum mechanics model presented earlier<sup>26</sup>. Briefly, to model the creep response, a solid disc geometry was used to describe a chondrocyte attached to a substrate. Studies in our laboratory using interferometry suggested this to be an appropriate approximation for the shape of a single chondrocyte<sup>28</sup>. With this geometry in mind, we considered the cell as a disc, under small deformation exposed to an instantaneous and constant load.

From the standard linear solid (Kelvin) model, and assuming the cell to be isotropic, incompressible, and homogeneous, the following solution was formulated to describe the viscoelastic creep response of a cell:

$$u_z(r, 0, t) = \frac{2\sigma}{3E_\infty} z(r, 0) \left[ 1 + \left( \frac{\tau_\epsilon}{\tau_\sigma} - 1 \right) e^{-\frac{t}{\tau_\sigma}} \right] H(t) \quad (1)$$

$$E_0 = E_\infty \left( \frac{\tau_\sigma}{\tau_\epsilon} \right)$$

$$\mu = E_\infty (\tau_\sigma - \tau_\epsilon)$$

where  $u_z$  is the deformation,  $\sigma$  is the contact stress,  $E_\infty$  is the relaxed modulus,  $z$  is the height of the cell,  $\tau_\sigma$  is the creep time constant,  $\tau_\epsilon$  is the stress relaxation time

constant,  $H(t)$  is the unit step function,  $E_0$  is the instantaneous modulus, and  $\mu$  is the intrinsic viscosity.

Creep experimentation generated three sets of data for each cell: displacement vs time, force vs time, and force vs displacement. The force vs time data were used to confirm constant force during testing, while the force vs displacement data were used to determine contact with the cell. The resulting creep curves were fitted and material properties were generated for the viscoelastic model via the non-linear Levenburg-Marquardt method, using MATLAB 6.5 (The MathWorks Inc., Natick, MA).

#### FLUORESCENCE MICROSCOPY: F-ACTIN STAINING

To compare the filamentous actin (F-actin) distribution and organization, all treatment groups (Table I) were stained with rhodamine phalloidin. Fluorescent derivatives of phallotoxins have been demonstrated to specifically bind to filamentous, but not to globular actin (G-actin)<sup>29</sup>. A number of studies have used fluorescently modified phallotoxins to quantify the amount of F-actin through fluorescent measurements, including image analysis<sup>30-33</sup>. Chondrocytes were seeded using the protocol above, except they were cultured on 24 × 30 mm tissue culture treated Thermanox plastic coverslips (Nalge Nunc International, Naperville, IL). Silicon isolators and the same cell density were used for seeding. After the culture period, cells were washed twice with phosphate buffered saline (PBS) warmed to 37°C. The cells were then fixed with fresh 3.7% paraformaldehyde for 10 min at room temperature, washed three times with PBS, and then permeabilized in 0.1% Triton X-100 in PBS for 5 min. After three more PBS washes, the fixed cells were incubated in rhodamine phalloidin (2 U per coverslip; Molecular Probes, Eugene, OR) in 1% bovine serum albumin (BSA) in PBS for 20 min, followed by three final washes with PBS. Each Thermanox coverslip was mounted between a microscope slide and glass coverslip using ProLong Gold with 4-6-diamidino-2-phenylindole (Molecular Probes, Eugene, OR). These samples were viewed with an Axioplan 2 microscope (Carl Zeiss, Oberkochen, Germany) and a CoolSNAP<sub>HQ</sub> CCD camera (Photometrics, Tucson, AZ). Images were acquired and analyzed using Metamorph 4.15 (Universal Imaging Corp., Downingtown, PA). All images were acquired in grayscale and colorized for presentation using Metamorph. For comparison of staining intensity, light exposure was kept to a minimum, and exposure time for digital photographs was kept at 30 ms. Overlaying and image processing were accomplished with Adobe Photoshop 7.0 (Adobe Systems, Inc., San Jose, CA).

The relative intensity of F-actin was determined for multiple cells in each treatment group using Metamorph to analyze the raw images. A region of interest was selected around a single cell and from this an average intensity (gray value) was obtained. The same size region was also selected over a nearby area without any cells to obtain a reading for the background fluorescence. The difference of these numbers was the cell's relative staining intensity. Average gray value (AGV) in a region of interest was determined with the following equation: AGV = total of all gray values/the total number of pixels. No threshold was set in the measurement of AGV for this analysis.

#### GENE EXPRESSION OF $\beta$ -ACTIN

Generally speaking, in healthy non-muscle tissue two isoforms ( $\beta$ - and  $\gamma$ -) of actin exist within a cell. Although little is

known about the exact functions of each isoform,  $\beta$ -actin and  $\gamma$ -actin have been associated with numerous microfilament structures and  $\beta$ -actin has been implicated in cell migration and cell motility. Previous studies have demonstrated higher densities of  $\beta$ - as compared to  $\gamma$ -isoform in cells, especially at the cell periphery and in lamella and filopodia<sup>34–37</sup>. Based on these findings, analysis of  $\beta$ -actin gene expression was selected for study due to its possible involvement in cell attachment and spreading.

Populations of  $2 \times 10^5$  chondrocytes were seeded in 24 well TCP plates. Each treatment group was represented in triplicate, yielding 48 samples. After 3 and 18 h of attachment, samples were lysed and their RNA was isolated using the RNAqueous kit (Ambion, Austin, TX). Total RNA concentration and purity were measured by a NanoDrop ND-1000 spectrophotometer (NanoDrop Technologies, Wilmington, DE), which allowed standardization by total RNA for the reverse transcription (RT) reaction. Before the RT reaction, RNA was subjected to DNase treatment. For the RT reaction, 38  $\mu$ L of RNA was incubated with oligo(dT) primer at 65 °C for 5 min. After cooling to room temperature, a 50  $\mu$ L reaction product was incubated with the RNA-oligo(dT) mix, buffer, 4 mM dNTPs (1 mM each dNTP), 40 U RNase inhibitor, and 50 U Stratagene StrataScript RT enzyme (La Jolla, CA) for 60 min at 42 °C. After cDNA synthesis, real-time PCR amplification for  $\beta$ -actin was performed using a RotorGene 3000 machine (Corbett Research, Sydney, Australia). A forward primer, reverse primer, and gene-specific probe were used. The 5' to 3' sequences for the forward primer (GACCAGATCATGTTCCAGA), reverse primer (CCAGAGGCGTACAGAGAC), and probe (ACTCCTGCCATGTATGTGGCCATC) were designed from bovine and human mRNA sequences from the National Center for Biotechnology Information (NCBI). The probe chemistry used in PCR reactions was 5' FAM and 3' BHQ-1. For real-time PCR analysis of each sample, 1  $\mu$ L of DNA sample, buffer, 3.5 mM MgCl<sub>2</sub>, 0.2 mM dNTPs, 100 nM of each forward and reverse primer, 100 nM probe, and 0.625 U HotStarTaq (Qiagen, Valencia, CA) were prepared in a 25  $\mu$ L reaction volume. The real-time analysis involved a 15 min activation step, followed by 50 cycles of 15 s at 95 °C, 30 s at 60 °C, and a fluorescence measurement.

The calculation of mRNA abundance of  $\beta$ -actin for all sample groups was facilitated by normalization with respect to total RNA concentration into the RT reaction. Abundance ( $A$ ) was calculated from the take-off cycle ( $C_T$ ) of  $\beta$ -actin and the efficiency ( $E$ ) of the reaction determined from a standard curve. The abundance equation used (adapted from Pfaffl)<sup>38</sup> is:

$$A = \frac{1}{(1 + E)^{C_T}} \quad (2)$$

The abundance was used to compare the expression of  $\beta$ -actin in all treatment groups.

#### DATA/STATISTICAL ANALYSIS

All results are reported as mean  $\pm$  standard deviation. *A priori* power analysis calculated a sample size of  $n = 22$  for the unconfined compression portion of this study. For the power analysis, a significance level of 0.05, a power of 0.8, and a difference of 30% were used. Estimates of cell mechanical properties and standard deviations were made using previous results. After sample sizes reached appreciable numbers, it became apparent that

the instantaneous and relaxed moduli were showing a difference of 40–50% between treated groups and, thus, a sample size of  $n = 11$  was chosen for the creep testing. Statistical analysis of the data was performed using JMP IN 5.1 (SAS Institute Inc., Cary, NC). The effects of zone, attachment time, and growth factor treatment were tested with three-factor ANOVA. The significance of these factors was determined for single cell mechanical properties, cell morphology (height and diameter) measurements, fluorescent intensity, and gene abundance. Where ANOVA revealed differences, a Tukey's Honestly Significant Difference (HSD) *post hoc* test was performed to make pair-wise comparisons among means.

## Results

### VISCOELASTIC PROPERTIES

An example of a typical creep curve from a single cell is presented in Fig. 1. This viscoelastic response was demonstrated by all 240 cells that were tested. These creep data were separately curve fit using Eq. (1) such that the instantaneous modulus, relaxed modulus, and apparent viscosity were determined for each treatment. A summary of the mean material properties ( $E_\infty$ ,  $E_0$ ,  $\mu$ ) is presented in Fig. 2. Compression with a test load of 50 nN did not appear to change cell area during testing or the calculation of contact stress. Experimentation required 15 animals and statistical analysis showed that animal was not a significant factor for any cell property ( $E_\infty$ ,  $E_0$ ,  $\mu$ , cell diameter, and cell height).

Three-factor ANOVA with *post hoc* analysis showed that each growth factor treatment (TGF- $\beta$ 1, IGF-I, and TGF- $\beta$ 1 + IGF-I) was a significant factor compared to no growth factor treatment for both the relaxed modulus [Fig. 2(A),  $P < 0.0001$ ] and instantaneous modulus [Fig. 2(B),  $P < 0.0001$ ]. Individual growth factor treatments were not statistically different from each other, and synergism was not observed from the combination of TGF- $\beta$ 1 + IGF-I. Growth factor treatment increased the relaxed modulus by 86% over controls and increased the instantaneous modulus by 136%. Furthermore, the combination of TGF- $\beta$ 1 and IGF-I significantly increased the apparent viscosity [Fig. 2(C)] by 45% over controls ( $P = 0.01$ ). Attachment time did not have a significant effect on instantaneous

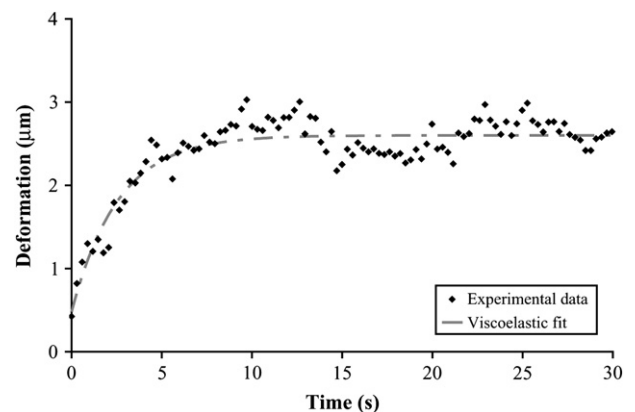


Fig. 1. Creep curve from a single chondrocyte, representing a typical viscoelastic response. The viscoelastic curve fit is included (dashed gray line).

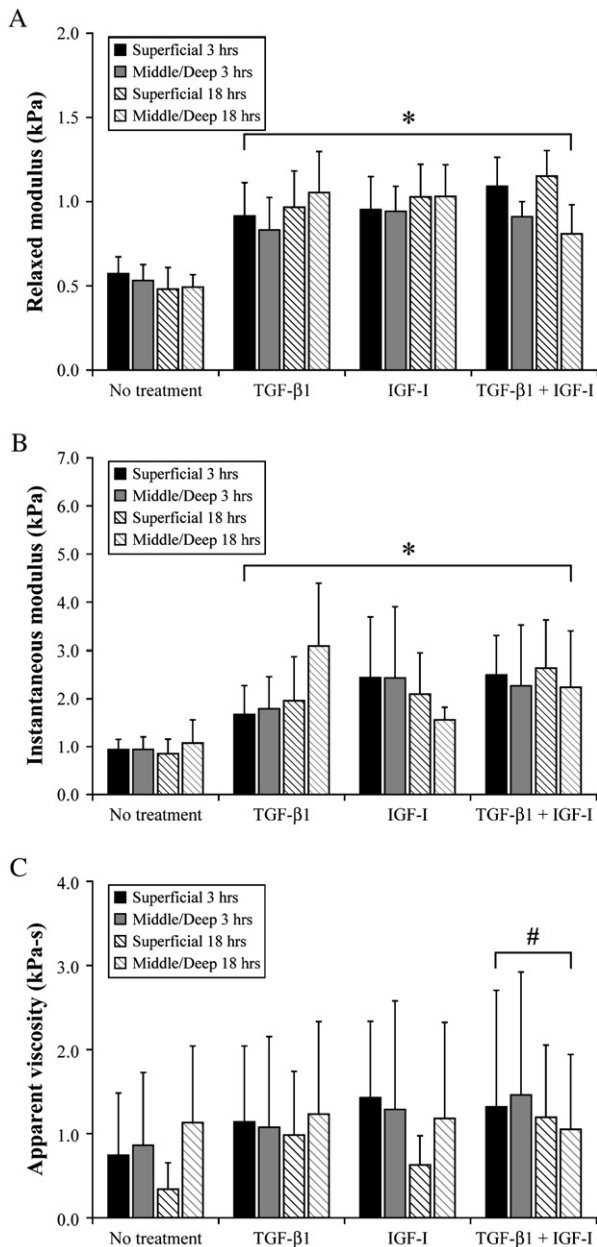


Fig. 2. Viscoelastic properties of single articular chondrocytes as a function of growth factor treatment, zone, and seeding time. The relaxed modulus (A) and instantaneous modulus (B) were significantly greater for growth factor treated chondrocytes as compared to controls ( $*P < 0.0001$ ). The combination of TGF- $\beta$ 1 + IGF-I significantly increased the apparent viscosity (C) over controls ( $\#P = 0.01$ ) but not compared to other growth factor treatments. Values of  $n$  ranged from 13 to 20.

modulus ( $P = 0.57$ ), relaxed modulus ( $P = 0.17$ ), or apparent viscosity ( $P = 0.06$ ). ANOVA also revealed that zone was a significant factor on the relaxed modulus ( $P = 0.0025$ ), with superficial cells having a total mean relaxed modulus ( $0.91 \pm 0.28$  kPa) that was 11% larger than middle/deep cells ( $0.82 \pm 0.25$  kPa). The interaction of zone and growth factor treatment was significant for the relaxed modulus ( $P < 0.0001$ ) and *post hoc* analysis revealed that superficial  $\times$  (TGF- $\beta$ 1 + IGF-I) resulted in significantly higher relaxed moduli than middle/deep  $\times$  (TGF- $\beta$ 1 + IGF-I) and

all other interactions [Fig. 2(A),  $P < 0.05$ ]. This zone  $\times$  growth factor interaction may have leveraged the effect of zone in the statistical analysis of the relaxed modulus.

Cells appeared more spread at 18 h, as demonstrated by smaller heights and greater diameters than cells at 3 h. After 3 h of attachment, cells had an average height of  $7.40 \pm 2.15$   $\mu$ m and an average diameter of  $11.94 \pm 1.21$   $\mu$ m. In comparison, after 18 h attachment cell height was  $6.09 \pm 1.93$   $\mu$ m and cell diameter was  $13.00 \pm 1.34$   $\mu$ m. ANOVA showed significant effects of attachment time with cell height decreasing from 3 to 18 h ( $P < 0.0001$ ) and cell diameter increasing from 3 to 18 h ( $P < 0.0001$ ). Additionally, chondrocytes treated with growth factors (TGF- $\beta$ 1, IGF-I, and TGF- $\beta$ 1 + IGF-I) had significantly greater cell heights as compared to control cells ( $P < 0.0001$ ) but were not significantly different from each other. At 3 h, growth factor treatment led to an average cell height of  $7.86 \pm 2.07$   $\mu$ m compared to control cells at  $6.00 \pm 1.76$   $\mu$ m. For growth factor treatment at 18 h of attachment, cell height was  $6.60 \pm 1.84$   $\mu$ m, whereas that of controls was  $4.42 \pm 1.11$   $\mu$ m. Three-factor ANOVA revealed that growth factor treatment was a significant factor on cell diameter ( $P = 0.003$ ). Growth factor treatment led to smaller cell diameters ( $12.22 \pm 1.24$   $\mu$ m) compared to control cells ( $12.50 \pm 1.54$   $\mu$ m). Zone was not a significant factor for cell height or diameter.

#### ACTIN STAINING/FLUORESCENT INTENSITY

The results of cell staining with rhodamine phalloidin and DAPI for all treatment groups are presented in Fig. 3. Cell spreading increased from 3 to 18 h of seeding time as did the degree of actin organization. A majority of chondrocytes from the growth factor treatment groups [Fig. 3(E–P)] exhibited a brighter halo at the periphery of the cell as compared to control cells [Fig. 3(A–D)]. Images taken after 18 h of seeding (Fig. 3, left eight panels) showed larger cells with discernable stress fibers, which were not visible at 3 h (Fig. 3, right eight panels).

Seven to 10 fluorescent images of cells were taken from each treatment group at  $100\times$  magnification. Collectively, the images contained an average of 51 cells for each treatment group. Average relative intensity values were determined for each treatment. The average relative intensity values mirrored the creep compression results (Fig. 4) and *post hoc* analysis showed an 86% increase for each growth factor treatment over controls ( $P < 0.0001$ ). The TGF- $\beta$ 1 group also exhibited a significant decrease in fluorescent intensity in comparison to IGF-I and in comparison to TGF- $\beta$ 1 + IGF-I ( $P < 0.0001$ ). Fluorescence intensity decreased by 24% at 18 h attachment as compared to 3 h ( $P = 0.0004$ ).

#### $\beta$ -ACTIN GENE EXPRESSION

Real-time PCR analysis was completed in duplicate on 48 samples, a standard dilution curve (serial dilutions of stock DNA:  $10\times$ ,  $100\times$ ,  $1,000\times$ ,  $10,000\times$ ), and no-template controls (NTCs), requiring two runs on the RotorGene. NTC amplification was not observed and reaction efficiency for each run was 96% and 97%, respectively. The results of  $\beta$ -actin abundance (Fig. 5) did not show a significant effect for any growth factor treatment ( $P = 0.70$ ), attachment time ( $P = 0.09$ ), or zone ( $P = 0.54$ ). However, a significant interaction was seen for zone and attachment time ( $P < 0.0001$ ). This is due to the fact that superficial zone

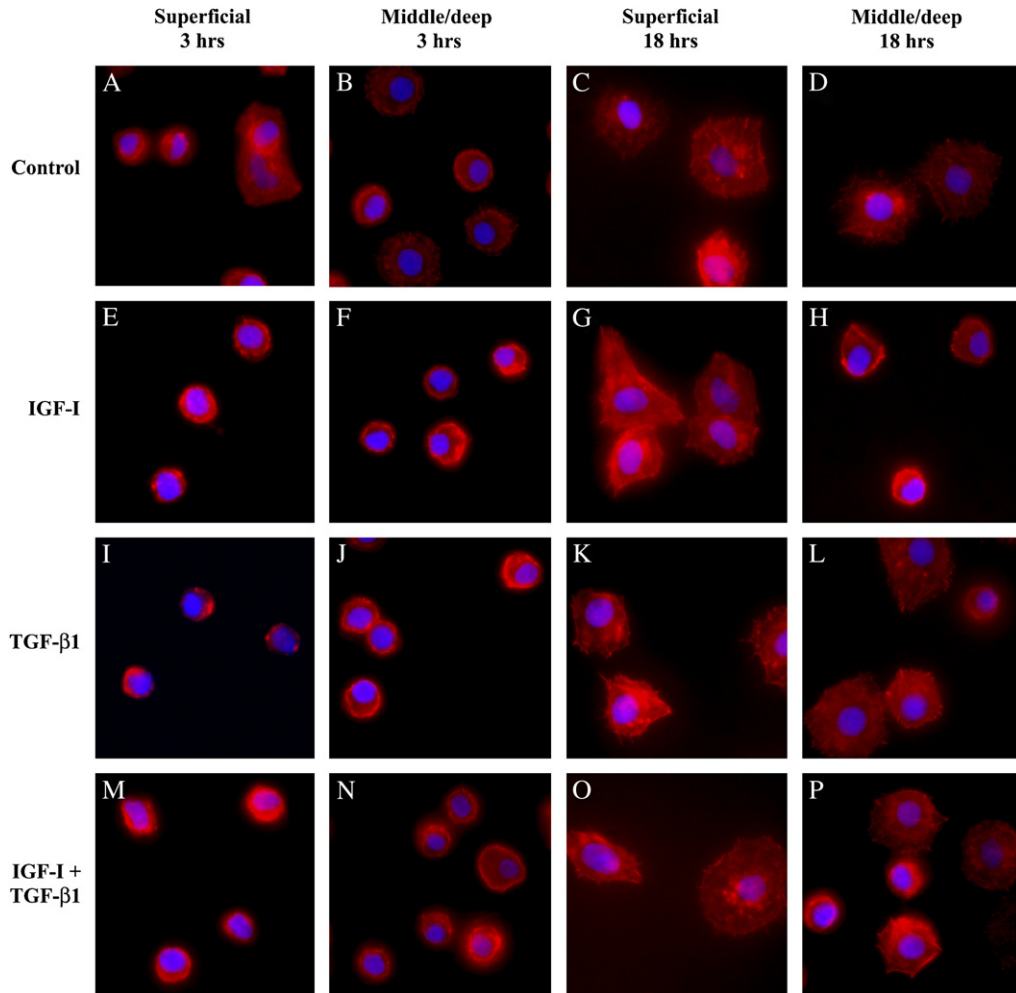


Fig. 3. Fluorescence images of each treatment group (100 $\times$ ). F-actin is stained with rhodamine phalloidin (red) and the nucleus is stained with DAPI (blue). Cells have more intense F-actin staining in growth factor groups and are less spread than control cells. Also, all groups show increased cell spreading from 3 to 18 h.

chondrocytes had a significantly lower ( $P < 0.0001$ ) abundance ( $2.80 \pm 0.76 \times 10^{-7}$ ) at 3 h as compared to 18 h ( $4.63 \pm 1.80 \times 10^{-7}$ ).

## Discussion

The unconfined creep compression results of this study demonstrate for the first time that the growth factors TGF- $\beta$ 1 and IGF-I, alone and in combination, significantly increase the stiffness of single zonal chondrocytes without synergistic effects observed between the two growth factors. Measurements of cell dimensions also demonstrate that these growth factor treatments alter the morphology of chondrocytes. The creep testing results further confirm that a viscoelastic model, assuming simple disc geometry, is suitable for modeling the response of a single chondrocyte to unconfined creep compression. This model also serves as a valuable tool for distinguishing the effects of growth factors on the mechanical properties of single cells. These findings yield important information toward understanding the process of mechanotransduction, which is gaining prominence as a crucial actor in tissue homeostasis and disease, as well as in the formation and maintenance of

cell phenotypes. Determination of single cell mechanical properties fosters understanding of a cell's local mechanical environment and that environment's role in shaping cellular physiology. Specifically for chondrocytes, it is important to understand the precise forces germane to tissue formation, and the etiopathogenesis of osteoarthritis, and how growth factors can modify these responses. Examination of single chondrocytes has already revealed important information in terms of relating mechanical properties to disease states<sup>39,40</sup>, cytoskeletal composition<sup>41</sup>, and the actions of growth factors<sup>21–23</sup>. This study adds to the current knowledge of growth factor effects on the cytoskeleton of single chondrocytes and provides insight to the study of basic cell functions.

The findings of this study demonstrate that separate techniques can be utilized to obtain similar information on the biomechanical nature of single chondrocytes. Creep compression of single chondrocytes showed mechanical stiffening induced by growth factors that corresponded with higher relative intensity measurements of chondrocytes stained with rhodamine phalloidin. These concomitant increases suggest that treatment with TGF- $\beta$ 1 and/or IGF-I increases the levels of F-actin within chondrocytes. This further implies that treatment with TGF- $\beta$ 1 and/or IGF-I leads to an

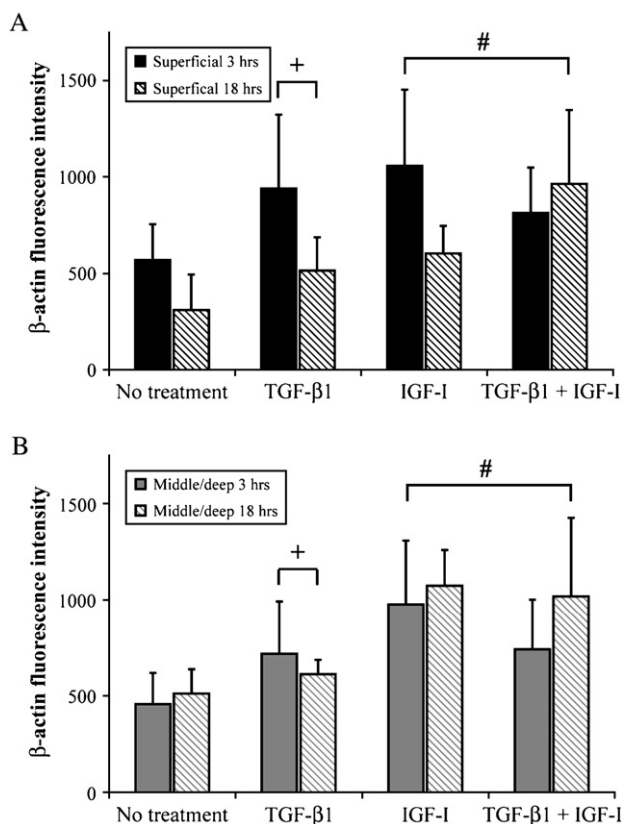


Fig. 4. Average fluorescence intensity of F-actin determined by fluorescent microscopy for superficial zone chondrocytes (A) and middle/deep zone chondrocytes (B). Results are presented as average  $\pm$  standard deviation. Plus (+) indicates significance over controls ( $P < 0.0001$ ), while # indicates significant over TGF- $\beta$ 1 and controls ( $P < 0.0001$ ). In general, there is agreement between the compressive modulus and F-actin intensity.

increase in the number of actin filaments with concomitant or subsequent cellular stiffening. Previous work has shown that actin microfilaments and possibly intermediate filaments contribute significantly to the biomechanical properties of single chondrocytes as measured by micropipette aspiration<sup>41</sup>. Also, TGF- $\beta$ 1 and IGF-I have previously been shown to increase the attachment of chondrocytes when compared to serum free controls<sup>23,42</sup>, suggesting increased focal adhesions and greater actin organization due to growth factor exposure. The growth factor treatments used in this study appear to affect cell stiffening in a similar manner, since analogous results were seen in all growth factor groups. Growth factor stimulation seems to be necessary for increases in F-actin as well as for cell stiffening to occur, since cells seeded for 3 and 18 h that were not exposed to growth factors did not show increased levels of F-actin or any cell stiffening. Further, synergistic effects were not observed when chondrocytes were stimulated with both TGF- $\beta$ 1 and IGF-I. These observations suggest the possibility of a common, yet currently unknown, mechanism.

The cell stiffening and increased F-actin that chondrocytes exhibited after TGF- $\beta$ 1 and IGF-I exposures most likely involve a gene and/or protein response within single cells. These growth factors have a well documented effect on gene expression<sup>8,10,19</sup>; therefore, the stiffening mechanism may involve transcriptional changes of

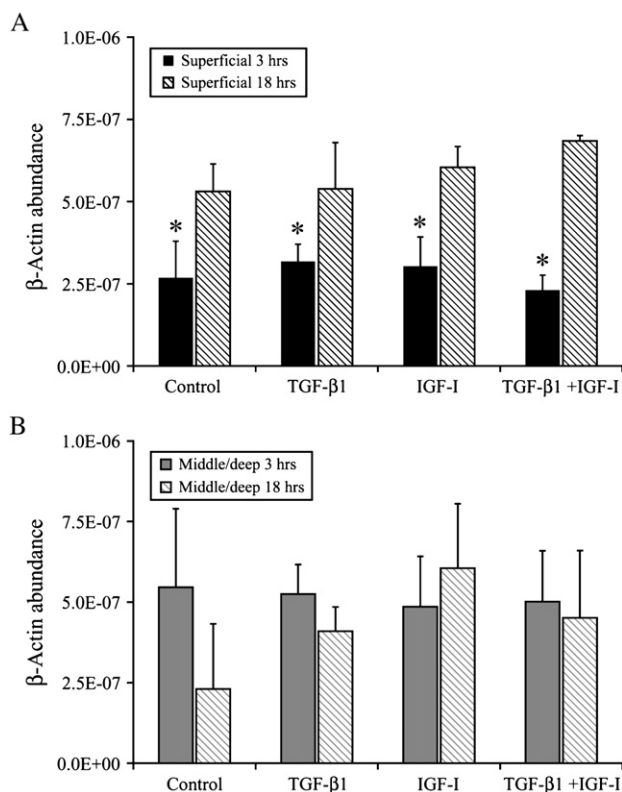


Fig. 5.  $\beta$ -Actin mRNA abundance in superficial (A) and middle/deep (B) chondrocytes. Results are presented as average  $\pm$  standard deviation. Asterisk (\*) indicates significance of 3 h as compared to 18 h for superficial zone ( $P < 0.0001$ ).

cytoskeletal and cytoskeletal related proteins. However, this does not appear to be the case since the expression of  $\beta$ -actin, as measured by real-time RT-PCR, demonstrates that TGF- $\beta$ 1 and IGF-I do not significantly increase mRNA levels for  $\beta$ -actin. We speculate that this may indicate that the pool of monomeric actin (G-actin) available for polymerization may not be increasing from direct transcription of the actin gene. Even though  $\beta$ -actin gene expression does not increase with growth factor treatment, translational regulation of G-actin levels may be occurring. A likely candidate could include eukaryotic initiation factor 2A (eIF2A) which has been demonstrated to regulate protein translation and is important in actin cytoskeletal organization in yeast<sup>43</sup>. These findings suggest that the observed response of chondrocytes to TGF- $\beta$ 1 and IGF-I is most likely occurring somewhere at the protein level. Previous research concerning chondrocytes, integrin activation, and stimulation by TGF- $\beta$ 1 or IGF-I has shown that signaling between focal adhesion complexes and growth factor receptors may occur<sup>21–23</sup>. For IGF-I it is clear that an Shc and Shc-GRB2 complex are important intermediates for linking to the MAPK pathway<sup>23</sup>. Current research has not yet revealed intermediate proteins connecting TGF- $\beta$ 1 and integrins to cell signaling or specifically Smad signaling. The increases in F-actin and cell stiffening seen in this study most likely involve intracellular signaling proteins that localize at focal adhesions as well as adaptor proteins.

Zonal differences in articular cartilage and isolated chondrocytes have been well characterized, not only in gene expression and synthesis<sup>44–46</sup>, but also in mechanical

properties. Several findings in this study further confirm that superficial chondrocytes differ physiologically from middle/deep chondrocytes. These data are in agreement with results from a recent study in our laboratory<sup>27</sup> that showed biomechanical differences between superficial and middle/deep chondrocytes. The real-time PCR results for expression of  $\beta$ -actin also illustrate differential responses of superficial and middle/deep cells during cell attachment. These results suggest that  $\beta$ -actin does not serve as a desirable housekeeping gene for chondrocytes, since expression is not constant across all treatments. As Fig. 5 shows, middle/deep chondrocytes maintain a relatively constant level of  $\beta$ -actin expression from 3 to 18 h of attachment time, while superficial chondrocytes have a lower level of  $\beta$ -actin expression at 3 h. By 18 h  $\beta$ -actin expression increases to a level equal to that of middle/deep chondrocytes at both 3 and 18 h attachment. This may be due to a differential response of superficial cells as compared to middle/deep cells when cells are digested from tissue and plated. The lower abundance of  $\beta$ -actin mRNA at 3 h does not seem sufficient to affect either the mechanical properties or the amount of F-actin in superficial chondrocytes. Some explanation can be garnered from previous work that has demonstrated that differences exist in the organization and the quantities of both actin and vimentin in zonal chondrocytes. Zonal differences have been observed in actin microfilament organization *in vivo* and in cells grown in monolayer<sup>47–49</sup> as well as in vimentin filament assembly and disassembly during organ culture<sup>47</sup>. It is interesting to note that zonal differences in cell morphology were not observed in this study. If chondrocytes exhibited similar morphologies to what is seen *in situ*, one would expect superficial cells to exhibit smaller cell heights and larger cell diameters than middle/deep zone cells. It appears that collagenase digestion followed by seeding in monolayer may alter the cytoskeleton such that morphologic differences between zonal cells no longer exist.

In contrast to studies with other cell types, attachment time did not play a factor in increasing chondrocyte stiffness as measured by single cell creep compression. The mechanical testing results of this study confirm a previous study from our group that demonstrated no significant effect of attachment time on any of the material properties of single chondrocytes as determined with the same creep testing device<sup>27</sup>. In contrast, fluorescence intensity of F-actin decreased from 3 to 18 h (Fig. 4). Decreased intensity measurements most likely are due to a diminished actin polymerization front, since less of a bright halo was seen in fluorescent staining of single cells at 18 h of attachment (Fig. 3). This may suggest that chondrocytes at 3 h have a denser network of actin microfilaments at the cell periphery where the cell is actively attaching and spreading. Previous research has correlated increases in cell stiffness with increased cell spreading and ECM contacts in bovine endothelial cells tested by twisting attached magnetic beads on the cell surface<sup>50,51</sup>. These differing behaviors can be attributed to cell type. Bovine articular chondrocytes do not adhere as easily as endothelial cells; at 3 h of attachment, chondrocytes remain round and are not firmly attached. Many of these cells can be detached by prodding with the compression probe or by a harsh PBS wash. At 18 h, chondrocytes are just starting to spread; however, a large percentage of rounded cells remain. There may be a threshold number of focal adhesions required to significantly stiffen a cell; therefore, attachment times greater than 18 h could show increased chondrocyte spreading and possibly increased cell stiffening.

We propose that the combination of integrin activation from cellular attachment and stimulation with TGF- $\beta$ 1 and IGF-I leads to increased actin polymerization as characterized by increases in F-actin and stiffening of the cytoskeleton. The increased polymerization is most likely due to signaling between integrins and growth factor receptors. These findings offer important information for cartilage

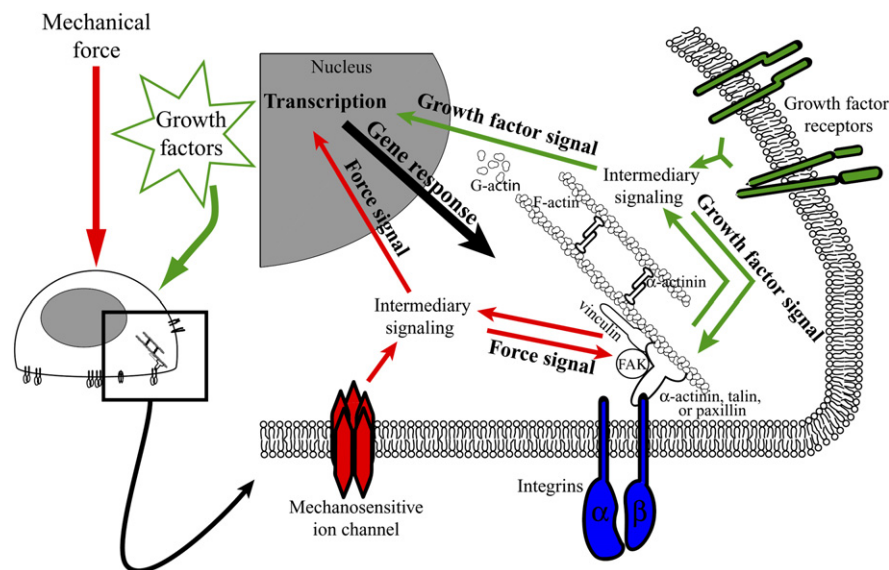


Fig. 6. Mechanical and growth factor stimulation in single cells. Growth factors have been shown to affect nuclear and integrin/focal adhesion signaling (right side of figure). Mechanical forces can be sensed by a variety of cellular proteins, such as mechanosensitive ion channels and integrins. These forces have also been shown to affect nuclear and integrin/focal adhesion signaling (left side of figure). Our group hopes to determine the interplay that may exist when cells are exposed to both stimuli.



physiology, tissue engineering of articular cartilage, and osteoarthritis. The activation of integrins through ECM binding and cross-talk with growth factor receptors might be a crucial process *in vivo*, especially for cartilage regeneration. The results of this study demonstrate that 3 h of TGF- $\beta$ 1 and IGF-I exposures cause significant changes to the actin cytoskeleton of single chondrocytes. This response may be short term or may continue with prolonged growth factor exposure. It is possible that cytoskeletal stiffening is part of a chondrocyte's preparation for the increased synthetic or proliferative activities that have been observed previously in populations of these cells. Our group is particularly interested in understanding how mechanical forces and growth factors affect processes in single chondrocytes (Fig. 6). This study establishes that by administering a characterized mechanical testing environment to single chondrocytes, their biomechanical response to external stimuli, such as growth factors, can be determined. The next step is to use this knowledge to correlate changes in gene expression and signaling with the direct compression of single chondrocytes. Growth factor stimulation surely plays a role in this response and may offer synergistic effects with certain modalities of mechanical stimulation. For cartilage, such synergism may influence tissue regeneration or inhibit damage/disease states caused by injurious mechanical loading. Connecting the application of force to changes in cell gene expression and signaling has broad implications; not only for the study of mechanotransduction, but for understanding disease etiologies and the formation or regeneration of tissues.

### Acknowledgments

This research was supported by an Osteoarthritis Biomarkers Biomedical Science Grant from the Arthritis Foundation and the National Institutes of Health Grant 5T32-GM008362.

### References

- Leipzig ND, Athanasiou KA. Cartilage regeneration. In: Wnek G, Bowlin G, Eds. *The Encyclopedia of Biomaterials and Bioengineering*. New York: Marcel Dekker Inc 2004:283–291.
- Sah RL, Kim YJ, Doong JY, Grodzinsky AJ, Plaas AH, Sandy JD. Biosynthetic response of cartilage explants to dynamic compression. *J Orthop Res* 1989;7: 619–36.
- Quinn TM, Grodzinsky AJ, Buschmann MD, Kim YJ, Hunziker EB. Mechanical compression alters proteoglycan deposition and matrix deformation around individual cells in cartilage explants. *J Cell Sci* 1998;111: 573–83.
- Hall AC, Urban JP, Gohl KA. The effects of hydrostatic pressure on matrix synthesis in articular cartilage. *J Orthop Res* 1991;9:1–10.
- Smith RL, Rusk SF, Ellison BE, Wessells P, Tsuchiya K, Carter DR, *et al.* *In vitro* stimulation of articular chondrocyte mRNA and extracellular matrix synthesis by hydrostatic pressure. *J Orthop Res* 1996;14:53–60.
- Buschmann MD, Gluzband YA, Grodzinsky AJ, Hunziker EB. Mechanical compression modulates matrix biosynthesis in chondrocyte/agarose culture. *J Cell Sci* 1995;108:1497–508.
- Vunjak-Novakovic G, Martin I, Obradovic B, Treppo S, Grodzinsky AJ, Langer R, *et al.* Bioreactor cultivation conditions modulate the composition and mechanical properties of tissue-engineered cartilage. *J Orthop Res* 1999;17:130–8.
- Gal era P, Vivien D, Pronost S, Bonaventure J, R edini F, Loyau G, *et al.* Transforming growth factor-beta 1 (TGF-beta 1) up-regulation of collagen type II in primary cultures of rabbit articular chondrocytes (RAC) involves increased mRNA levels without affecting mRNA stability and procollagen processing. *J Cell Physiol* 1992;153:596–606.
- Rosen DM, Stempien SA, Thompson AY, Seyedin SM. Transforming growth factor-beta modulates the expression of osteoblast and chondroblast phenotypes *in vitro*. *J Cell Physiol* 1988;134:337–46.
- Frazier A, Bunning RA, Thavarajah M, Seid JM, Russell RG. Studies on type II collagen and aggrecan production in human articular chondrocytes *in vitro* and effects of transforming growth factor-beta and interleukin-1beta. *Osteoarthritis Cartilage* 1994;2: 235–45.
- Malemud CJ, Killeen W, Hering TM, Purchio AF. Enhanced sulfated-proteoglycan core protein synthesis by incubation of rabbit chondrocytes with recombinant transforming growth factor-beta 1. *J Cell Physiol* 1991; 149:152–9.
- Qi WN, Scully SP. Effect of type II collagen in chondrocyte response to TGF-beta 1 regulation. *Exp Cell Res* 1998;241:142–50.
- Bonassar LJ, Grodzinsky AJ, Srinivasan A, Davila SG, Trippel SB. Mechanical and physicochemical regulation of the action of insulin-like growth factor-I on articular cartilage. *Arch Biochem Biophys* 2000;379: 57–63.
- Bonassar LJ, Grodzinsky AJ, Frank EH, Davila SG, Bhaktav NR, Trippel SB. The effect of dynamic compression on the response of articular cartilage to insulin-like growth factor-I. *J Orthop Res* 2001;19:11–7.
- Gooch KJ, Blunk T, Courter DL, Sieminski AL, Bursac PM, Vunjak-Novakovic G, *et al.* IGF-I and mechanical environment interact to modulate engineered cartilage development. *Biochem Biophys Res Commun* 2001;286:909–15.
- Madry H, Zurakowski D, Trippel SB. Overexpression of human insulin-like growth factor-I promotes new tissue formation in an *ex vivo* model of articular chondrocyte transplantation. *Gene Ther* 2001;8:1443–9.
- Nixon AJ, Lillich JT, Burton-Wurster N, Lust G, Mohammed HO. Differentiated cellular function in fetal chondrocytes cultured with insulin-like growth factor-I and transforming growth factor-beta. *J Orthop Res* 1998;16:531–41.
- van Susante JL, Buma P, van Beuningen HM, van den Berg WB, Veth RP. Responsiveness of bovine chondrocytes to growth factors in medium with different serum concentrations. *J Orthop Res* 2000;18: 68–77.
- Yaeger PC, Masi TL, de Ortiz JL, Binette F, Tubo R, McPherson JM. Synergistic action of transforming growth factor-beta and insulin-like growth factor-I induces expression of type II collagen and aggrecan genes in adult human articular chondrocytes. *Exp Cell Res* 1997;237:318–25.
- Shieh AC, Athanasiou KA. Biomechanics of single chondrocytes and osteoarthritis. *Crit Rev Biomed Eng* 2002;30:307–43.

21. Lee JW, Hee Kim Y, Boong Park H, Xu LH, Cance WG, Block JA, *et al.* The C-terminal domain of focal adhesion kinase reduces the tumor cell invasiveness in chondrosarcoma cell lines. *J Orthop Res* 2003;21:1071–80.
22. Schneiderbauer MM, Dutton CM, Scully SP. Signaling “cross-talk” between TGF-beta1 and ECM signals in chondrocytic cells. *Cell Signal* 2004;16:1133–40.
23. Shakibaei M, John T, De Souza P, Rahmzadeh R, Merker HJ. Signal transduction by beta1 integrin receptors in human chondrocytes *in vitro*: collaboration with the insulin-like growth factor-I receptor. *Biochem J* 1999;342:615–23.
24. Shin D, Athanasiou K. Cytoindentation for obtaining cell biomechanical properties. *J Orthop Res* 1999;17:880–90.
25. Koay EJ, Shieh AC, Athanasiou KA. Creep indentation of single cells. *J Biomech Eng* 2003;125:334–41.
26. Leipzig ND, Athanasiou KA. Unconfined creep compression of chondrocytes. *J Biomech* 2005;38:77–85.
27. Shieh AC, Athanasiou KA. Biomechanics of single zonal chondrocytes. *J Biomech* (In press).
28. Scott CC, Luttge A, Athanasiou KA. Development and validation of vertical scanning interferometry as a novel method for acquiring chondrocyte geometry. *J Biomed Mater Res A* 2005;72:83–90.
29. Cooper JA. Effects of cytochalasin and phalloidin on actin. *J Cell Biol* 1987;105:1473–8.
30. Howard TH, Meyer WH. Chemotactic peptide modulation of actin assembly and locomotion in neutrophils. *J Cell Biol* 1984;98:1265–71.
31. Knowles GC, McCulloch CA. Simultaneous localization and quantification of relative G and F actin content: optimization of fluorescence labeling methods. *J Histochem Cytochem* 1992;40:1605–12.
32. Rao JY, Hurst RE, Bales WD, Jones PL, Bass RA, Archer LT, *et al.* Cellular F-actin levels as a marker for cellular transformation: relationship to cell division and differentiation. *Cancer Res* 1990;50:2215–20.
33. Lichtenstein N, Geiger B, Kam Z. Quantitative analysis of cytoskeletal organization by digital fluorescent microscopy. *Cytometry A* 2003;54:8–18.
34. DeNofrio D, Hooch TC, Herman IM. Functional sorting of actin isoforms in microvascular pericytes. *J Cell Biol* 1989;109:191–202.
35. Hooch TC, Newcomb PM, Herman IM. Beta actin and its mRNA are localized at the plasma membrane and the regions of moving cytoplasm during the cellular response to injury. *J Cell Biol* 1991;112:653–64.
36. Hofer D, Ness W, Drenckhahn D. Sorting of actin isoforms in chicken auditory hair cells. *J Cell Sci* 1997;110:765–70.
37. Watanabe H, Kislauskis EH, Mackay CA, Mason-Savas A, Marks SC Jr. Actin mRNA isoforms are differentially sorted in normal osteoblasts and sorting is altered in osteoblasts from a skeletal mutation in the rat. *J Cell Sci* 1998;111:1287–92.
38. Pfaffl MW. A new mathematical model for relative quantification in real-time RT-PCR. *Nucleic Acids Res* 2001;29:2002–7.
39. Trickey TR, Lee M, Guilak T. Viscoelastic properties of chondrocytes from normal and osteoarthritic human cartilage. *J Orthop Res* 2000;18:891–8.
40. Alexopoulos LG, Haider MA, Vail TP, Guilak F. Alterations in the mechanical properties of the human chondrocyte pericellular matrix with osteoarthritis. *J Biomech Eng* 2003;125:323–33.
41. Trickey WR, Vail TP, Guilak F. The role of the cytoskeleton in the viscoelastic properties of human articular chondrocytes. *J Orthop Res* 2004;22:131–9.
42. Loeser RF. Growth factor regulation of chondrocyte integrins. Differential effects of insulin-like growth factor 1 and transforming growth factor beta on alpha 1 beta 1 integrin expression and chondrocyte adhesion to type VI collagen. *Arthritis Rheum* 1997;40:270–6.
43. Komar AA, Gross SR, Barth-Baus D, Strachan R, Hensold JO, Goss Kinzy T, *et al.* Novel characteristics of the biological properties of the yeast *Saccharomyces cerevisiae* eukaryotic initiation factor 2A. *J Biol Chem* 2005;280:15601–11.
44. Aydelotte MB, Kuettner KE. Differences between sub-populations of cultured bovine articular chondrocytes. I. Morphology and cartilage matrix production. *Connect Tissue Res* 1988;18:205–22.
45. Aydelotte MB, Greenhill RR, Kuettner KE. Differences between sub-populations of cultured bovine articular chondrocytes. II. Proteoglycan metabolism. *Connect Tissue Res* 1988;18:223–34.
46. Darling EM, Hu JC, Athanasiou KA. Zonal and topographical differences in articular cartilage gene expression. *J Orthop Res* 2004;22:1182–7.
47. Durrant LA, Archer CW, Benjamin M, Ralphs JR. Organisation of the chondrocyte cytoskeleton and its response to changing mechanical conditions in organ culture. *J Anat* 1999;194:343–53.
48. Idowu BD, Knight MM, Bader DL, Lee DA. Confocal analysis of cytoskeletal organisation within isolated chondrocyte sub-populations cultured in agarose. *Histochem J* 2000;32:165–74.
49. Langelier E, Suetterlin R, Hoemann CD, Aebi U, Buschmann MD. The chondrocyte cytoskeleton in mature articular cartilage: structure and distribution of actin, tubulin, and vimentin filaments. *J Histochem Cytochem* 2000;48:1307–20.
50. Wang N, Butler JP, Ingber DE. Mechanotransduction across the cell surface and through the cytoskeleton. *Science* 1993;260:1124–7.
51. Wang N, Ingber DE. Control of cytoskeletal mechanics by extracellular matrix, cell shape, and mechanical tension. *Biophys J* 1994;66:2181–9.